In Vivo Estimation of Magnetization Transfer Rates Between White Matter Water Compartments

P van Gelderen, JH Duyn

Advanced MRI section, LFMI, NINDS, National Institutes of Health, Bethesda, MD, USA

Advanced MRI

Introduction

Magnetization transfer (MT) rates between protons in myelin solids (MS) and those in water can be studied by dedicated MRI experiments in which the proton magnetization levels are transiently altered by the use of RF inversion or saturation prepulses [1]. Here we combined various preparation pulses with a multi-gradient echo (MGRE) acquisition to distinguish between myelin water (MW), axonal- and interstitial water (OW) [2] to establish their MT kinetics [3], in analogy to T_2-based separation used previously [4]. To account for complexities in the distribution of water within the myelin sheath, a multi-compartment model including alternating layers of MS and MW was developed.

Theory

The analysis is based on a combination of a three-component fitting of the MRGE data, followed by the fitting of a multi-layer exchange (ML3) model illustrated in Fig. 1. The ML3-model is an extension of the three component model in that it adds solids, and it has multiple layers of MW and MS instead of one MW compartment. It also adds exchange between MW and MS, as well as exchange of water across the MS layers. To reduce the number of equations and parameters, the model was simplified by assuming that axonal and interstitial water behave sufficiently similar to consider them jointly, and thus simulate of only half of the total myelin sheath thickness with a single adjacent water compartment.

The three-component fitting was based on the analysis outlined in [2], fitting the following equation to the MGRE data:

$$S(t) = (a_1 e^{-R^*_{2,1}t + i\omega_1 t} + a_2 e^{-R^*_{2,2}t + i\omega_2 t} + a_3 e^{-R^*_{2,3}t}) e^{i(\omega_0 t + \phi_0)} \quad [1]$$

describing the signal as function of (echo) time as a sum of three exponential decays, each with an amplitude and decay rate, a global phase and frequency and a frequency offset for the first two. The three components are assumed to be myelin water, axonal water and interstitial water.

The ML3-model consisted of a set of Bloch equations for each compartment in the model (the individual MS and MW layers and the OW), coupled to each other by additional exchange terms. Considering only relaxation and exchange terms, the equations can be written as:

$$\frac{f_{MW}}{N}\frac{dM^{MW}_{z,i}}{dt} = -\frac{f_{MW}}{N}(1-M^{MW}_{z,i})R^{MW}_1 - (2k_{WW}+k_{WS})M^{MW}_{z,i} + k_{WW}(M^{MW}_{z,i-1}+M^{MW}_{z,i+1}) + k_{WS}M^{MS}_{z,i} \quad [2]$$

$$\frac{f_{MW}}{N}\frac{dM^{MW}_{xy,i}}{dt} = -\frac{f_{MW}}{N}M^{MW}_{xy,i}R^{MW}_2 - (2k_{WW}+k_{WS})M^{MW}_{xy,i} + k_{WW}(M^{MW}_{xy,i-1}+M^{MW}_{xy,i+1}) + k_{WS}M^{MS}_{xy,i} \quad [3]$$

$$\frac{f_{MS}}{N+1}\frac{dM^{MS}_{z,i}}{dt} = -\frac{f_{MS}}{N+1}(1-M^{MS}_{z,i})R^{MS}_1 - k_{WS}M^{MS}_{z,i} + k_{WS}M^{MW}_{z,i} \quad [4]$$

$$\frac{f_{MS}}{N+1}\frac{dM^{MS}_{xy,i}}{dt} = -\frac{f_{MS}}{N+1}M^{MS}_{xy,i}R^{MS}_2 - k_{WS}M^{MS}_{xy,i} + k_{WS}M^{MW}_{xy,i} \quad [5]$$

$$f_{OW}\frac{dM^{OW}_{z}}{dt} = -f_{OW}(1-M^{OW}_{z})R^{OW}_1 - (k_{WW}+k_{WS})M^{OW}_{z} + k_{WW}M^{MW}_{z,N} + k_{WS}M^{MS}_{z,N+1} \quad [6]$$

$$f_{OW}\frac{dM^{OW}_{xy}}{dt} = -f_{OW}M^{OW}_{xy}R^{OW}_2 - (k_{WW}+k_{WS})M^{OW}_{xy} + k_{WW}M^{MW}_{xy,N} + k_{WS}M^{MS}_{xy,N+1} \quad [7]$$

where N indicates the number of MW compartments , f the fraction of spins of one type (making f_{MW}/N the size of one myelin water layer), M_z and M_{xy} the longitudinal and transverse magnetization, R_1 and R_2 their relaxation rates, and k_{WW} and k_{WS} exchange rates as fraction of spins per unit time for exchange from water to water and between water and solids. The full set of equations used for the model included terms for B_0 and B_1 rotations to describe effects of off-resonance and all RF pulses, and some adjustments for the compartments at the ends (for i=0 and i=N) for Eq. 2 & 3.

Data Acquisition

Four types of scans with different RF preparation pulses were used:

REF) no preparation pulse (reference),
IR) a single inversion pulse aimed at OW inversion,
DI) MS saturation with double inversion with minimum interpulse delay,
DS) Selective OW saturation by double inversion with delay between the pulses.

Ten human subjects were scanned on a Siemens Magnetom 7T under IRB approved protocol. Five slices were acquired with a MGRE-type acquisition, each at five delay times. Acquisition parameters: 90x60 voxels, 240x160mm² FOV, 2mm slices, 90 degree flip-angle, 3s TR, except for type DS which used a TR of 1.5s, TE 2-46ms, 80 echoes. All inversion pulses were 10ms hyperbolic-secant pulses at 750Hz maximum B_1. A navigator was incorporated after echo 31 for frequency correction.

Analysis

A region of interest (ROI) was manually defined for every subject in the splenium of the corpus callosum. The complex image data was averaged in these ROIs after phase corrections [2]. The ROI averages were analyzed in two steps:

1) For each subject and scan type, the data was fitted with the three-compartment model (Eq. 1). The REF scan was fitted first, then the non-linear parameters where fixed and the data from the other scan types were fitted to obtain the amplitudes of the three components for all delay times. These amplitudes were then normalized by division with the corresponding amplitudes from the REF scan and the axonal and interstitial components were added to form the OW. Finally, these results were averaged over the subjects and standard errors (SE) were derived for each scan type. This resulted in 30 data points (5 delays, 3 scan types, 2 pools: MW and OW), as plotted in Fig. 2.

2) The ML3-model, as formulated in Theory, was fitted to the results of step 1. The fitting criterion was a χ^2-measure calculated as the sum of squares of the difference between the data and the model, divided by the SEs. The model was fitted by numerically solving the set of equations (Eq. 2-7), simulating the MR experiments, and optimizing the parameters to match the acquired data. The simulation included the effects of slice profiles and the RF pulses of all the slices (the off-resonance excitation pulses of other slices can change the state of the MS spins).
To limit the number of parameters to be determined in this step, several were fixed to values found in step 1, in particular in the three-component fit of the REF data. The fixed parameters were the R_2^* and frequency of MW and OW, and the ratio of their amplitudes (setting f_{MW}/f_{OW}). The frequency and R_2^* of MS were taken from [5]. Error analysis showed that the R_1^{MS} and R_1^{MW} could not separately be determined in this analysis, so they were replaced by a single parameter. Finally, the number of layers (N) could not be determined by fitting and so the model was fitted with four different fixed values for N (5,9,12 and 15).

To help characterize the results, two time constants were derived for each type of compartment: the exchange time (τ), defined as the volume of a single compartment divided by the sum of the relevant exchange rates; the exchange induced decay time (T), defined as the time it takes for the average M_z of all compartments of one type to decay by a factor of 1/e towards the equilibrium value when ignoring all relaxation effects.

Results

The average MW and OW signal as function of delay time for the three scan types is shown in Fig. 2, with the fitted curves from the ML3-model (with N=9). The model fitted the data well, although the χ^2 was four times higher than what would be expected for the ideal case (98 versus 25). Fig. 3 illustrates that while the individual layers can have a rather different M_Z evolution and this depends on N, the decay of the average of all MW is quite similar for different N. This also shows that N can not be determined with this model, since only the average signal of all layers is available as measured input. The calculated exchange times and exchange induced decay times (Table 1) reflect what is shown in Fig.3: the individual compartment exchange times depend on N, while the decay times of the averages are almost constant.

The best fit was with f_{MS}=0.25, R_1^{MS} & R_1^{MW}= 1.84/s, R_1^{OW}=0.36/s, $(N+1)k_{WS}$= 3.2/s, all independent of N; $(N+1)k_{WS}$ is the total exchange between water and solids, as there are N+1 MS compartments. Only k_{WW} depended on N, in a linear fashion, as k_{WW} =0.38+0.86N /s. The fixed parameters were: f_{MW}/f_{OW}= 0.14, R_2^{MS}=16/s, R_2^{MW}= 0.13/s, R_2^{OW}=0.033/s, MS frequency 700Hz, MW frequency 35Hz (0Hz for OW).

Discussion

The ML3-model forms a good fit for the averaged MGRE data in splenium of the corpus callosum. For a reasonable choice of N for this brain region with mostly 1µm-size fibers (N~9-12), the single layer exchange time is in the order of 500µs, consistent with previous permeability results [6-10]. The decay time for the total MW was 14ms, substantially shorter than the equivalent (69ms) calculated from [4]. As the exchange of MW with OW is fast compared to commonly used MRI TEs, this exchange, and the dispersion within the MW (T_2^*~7ms), can potentially play a role in many types of MRI, especially in T_2 or diffusion experiments with longer TEs. All pools appear well mixed on a T_1 time scale, which implies the T_1 as observed in the brain in a typical clinical MRI is dominated by the MS (and MW) pool, consistent with previous results [11-13]. The MS pool size and R_1's are consistent with [12-14].

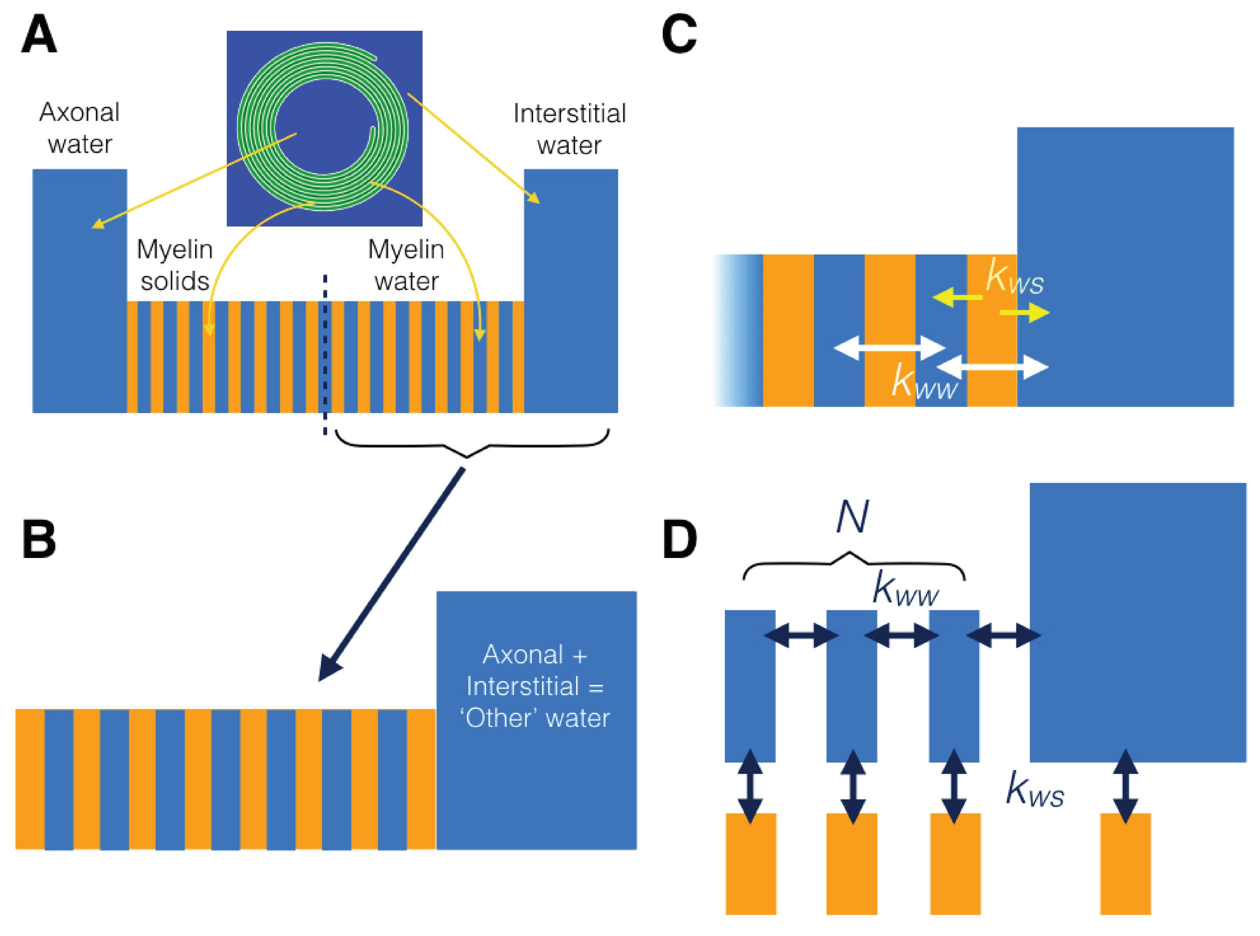

Figure 1: The multi-layer exchange model. A) Starting point: the 3 water pools with the addition of MS-layers; B) simplification: assuming axonal and interstitial water behave the same, allowing simulation of half the model by symmetry; C) the two exchange flows: between MS and the surrounding water (k_{WS}) and between water compartments (k_{WW}) across the MS layers; D) symbolic representation of the situation in C, clarifying the model by separation of the MS compartments from in between water compartments.

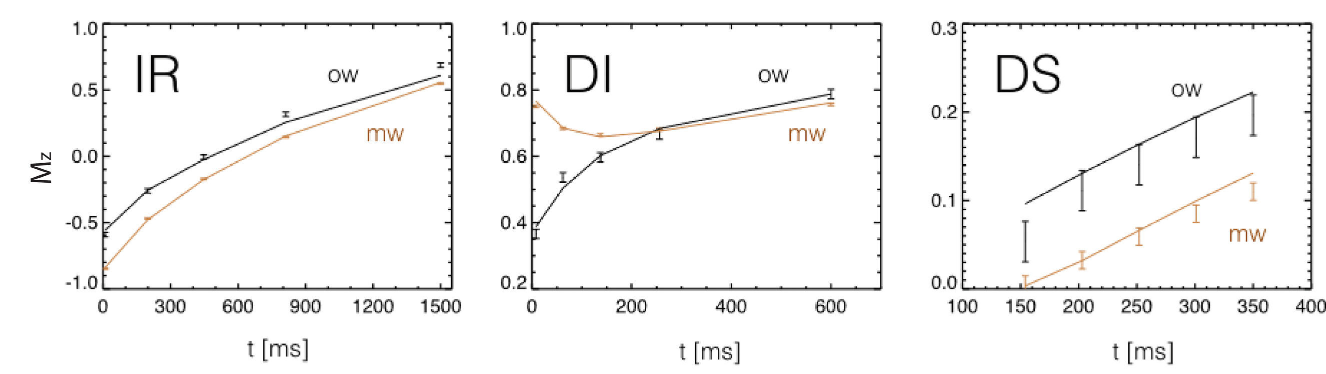

Figure 2: The ROI and subject averaged M_z for the two water components as function of delay time for three different scan types plotted as error bars (showing the SE) and the M_z simulated with the ML3-model, plotted as lines.

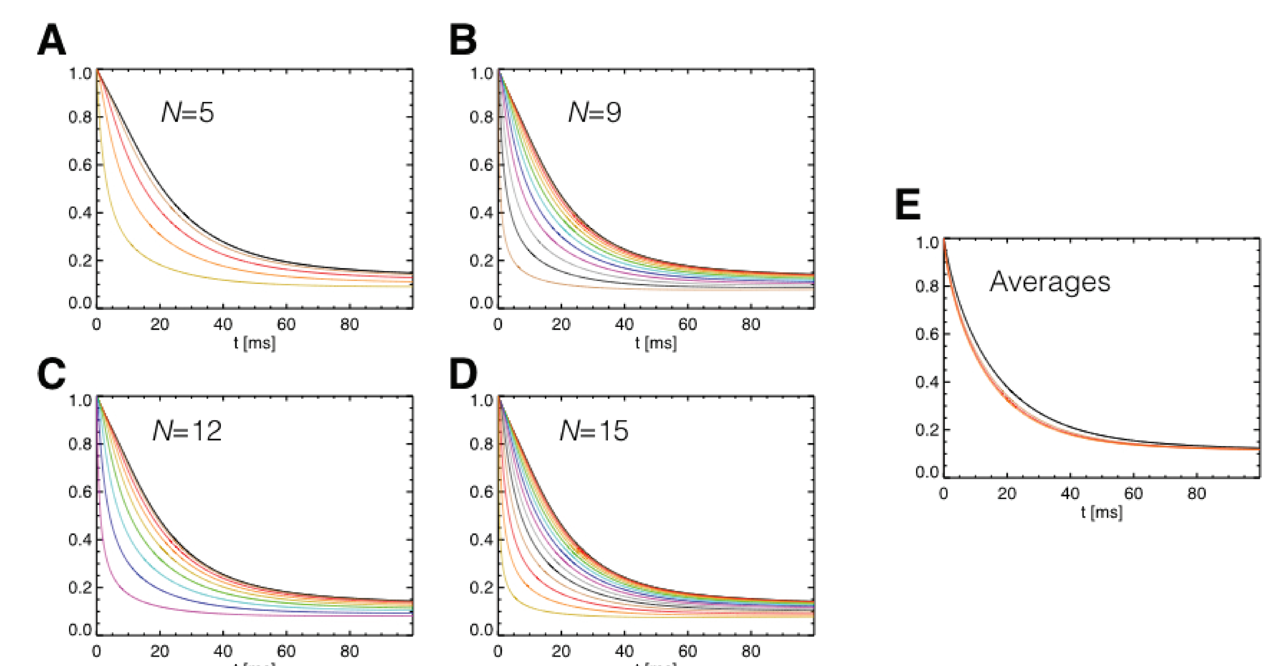

Figure 3: Simulation of the decay of M_z in the MW compartments, when starting with all $M_{z,i}^{MW}$=1 and the other compartments all at zero, while ignoring relaxation. A-D show the individual layers for models with N=5,9,12 and 15; E shows the averages over the MW compartments for the different N values.

Table 1: Exchange times (τ) and exchange induced decay times (T) in ms, calculated from the ML3-model for four choices of N.

N		5	9	12	15
τ	MS	84	80	78	77
	MW	1.83	0.61	0.34	0.22
	OW	128	78	60	50
T	MS	95.5	97.3	98.0	98.2
	MW	16.9	14.7	14.0	13.6
	OW	112	112	112	112

References

1) Gochberg DF et.al., Magn. Reson. Med. 1997:38:224.
2) Li X et.al., Neuroimage Clinical 2015:7:709.
3) Gochberg DF, Gore JC, Magn. Reson. Med. 2003:49:501.
4) Kalantari S et.al., Magn. Reson. Med. 2011:66:1142.
5) Jiang X,van Gelderen P, Duyn JH, ISMRM 2016:1502
6) Franks NP, Lieb WR, J. Mol. Biol. 1980:141:43
7) Conlon T, Outhred R, Biochim. BioPhys. Acta, 1978:511:408
8) Cass A, Finkelstein A, J. Gen. Physiol. 1967:50:1765
9) Finkelstein A, J. Gen. Physiol. 1976:68:127
10) Harkins KD, Dula AN, Does MD, Magn. Reson. Med. 2012:67:793
11) Koenig SH, Brown RD, Magn. Reson. Med., 1990:14:482
12) Fatouros PP, Marmarou A, J. Neurosurg. 1999:90:109
13) Rooney WD et.al., Magn. Resson. Med. 2007:57:308
14) van Gelderen P, Jiang X, Duyn JH, Neuroimage 2016:128:85

To download this poster please visit:
http://amri.ninds.nih.gov/presentations/2017/gelderen.wmml.pdf